Holocene climate forcings on leaf wax hydrogen isotope records in the monsoon regions of China

Xinxin Wang,[1] Xianyu Huang,[2,*] Yixiao Xue,[1] Jie Wu,[1] and Shucheng Xie[2]

*Correspondence: xyhuang@cug.edu.cn

Received: April 27, 2025; Accepted: September 23, 2025; Published Online: September 26, 2025; https://doi.org/10.59717/j.xinn-geo.2026.100180

GRAPHICAL ABSTRACT

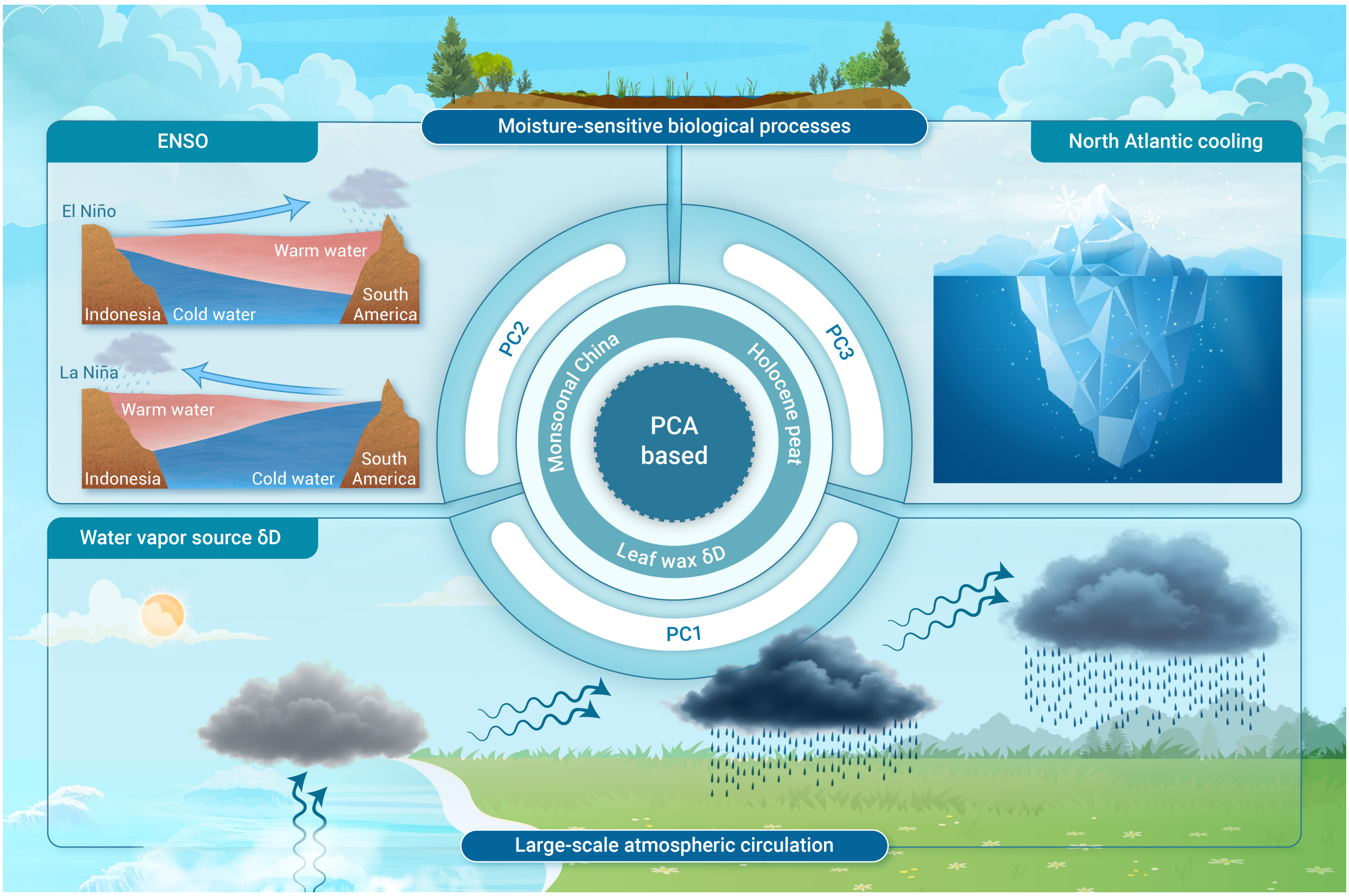

PUBLIC SUMMARY

- PCA on the Holocene peat leaf wax δD records from the monsoon regions of China.
- PC1 linked to the water vapor source isotopes.
- PC2 and PC3 related to the El Niño-Southern Oscillation (ENSO) and North Atlantic cooling, respectively.
- PC2 and PC3 mainly responsible for the spatial heterogeneity of precipitation.
- Moisture-sensitive biological effects likely differentiating leaf wax δD from stalagmite $\delta^{18}O$ records.

Holocene climate forcings on leaf wax hydrogen isotope records in the monsoon regions of China

Xinxin Wang,[1] Xianyu Huang,[2,*] Yixiao Xue,[1] Jie Wu,[1] and Shucheng Xie[2]

[1]State Key Laboratory for Vegetation Structure, Functions and Construction (VegLab), Institute of Palaeontology, Yunnan Key Laboratory of Earth System Science, Yunnan University, Kunming 650500, China

[2]State Key Laboratory of Geomicrobiology and Environmental Changes, Hubei Key Laboratory of Critical Zone Evolution, China University of Geosciences, Wuhan 430078, China

*Correspondence: xyhuang@cug.edu.cn

Received: April 27, 2025; Accepted: September 23, 2025; Published Online: September 26, 2025; https://doi.org/10.59717/j.xinn-geo.2026.100180

Citation: Wang X., Huang X., Xue Y., et al. (2026). Holocene climate forcings on leaf wax hydrogen isotope records in the monsoon regions of China. *The Innovation Geoscience* **4**:100180.

The hydrogen isotopic compositions (δD) of leaf waxes have emerged as a pivotal paleohydrological proxy. However, their complex nature complicates paleoclimatic interpretations in the monsoon regions of China. To disentangle the controls, we performed principal component analysis (PCA) on Holocene leaf wax δD records from peat deposits across the monsoon regions of China, which reveals three dominant signals. The first principal component (PC1) strongly correlates with water vapor source isotopes. The second principal component (PC2) shows a close relationship with El Niño-Southern Oscillation (ENSO) mean state. The third principal component (PC3) is associated with North Atlantic cooling. Together, PC2 and PC3 mainly account for the spatiotemporal variations of precipitation in the monsoon regions of China. The PCA results highlight that while Northern hemisphere solar insolation provides the fundamental control, both high- and low-latitude climate systems modulate the isotopic signals. Moreover, these findings offer new insights into resolving the discrepancies between leaf wax δD and stalagmite $\delta^{18}O$ records in the Asian monsoon regions during the Holocene. Given the observed covariation between PC1 and stalagmite $\delta^{18}O$ records, we tentatively attribute the differences to moisture-dependent biological factors significantly affecting leaf wax δD.

INTRODUCTION

The stable hydrogen and oxygen isotopic compositions (δD and $\delta^{18}O$, respectively) in precipitation, are uniquely positioned to track hydrological changes. The power of these isotopes mainly lies in three aspects: (1) Tracing water sources through isotopic fractionation during atmospheric transport, (2) resolving hydrological processes underrepresented in conventional proxies, and (3) synthesizing hydrological signals across spatiotemporal scales.[1] These isotopic fingerprints are ultimately registered in continental geological repositories, including stalagmites, ice cores, and limnic sediments, providing critical insights into past hydroclimatic regimes.

Among these archives, leaf wax δD has emerged as an excellent paleohydrological proxy. Its strengths are threefold: A robust global correlation with precipitation δD,[2,3] exceptional preservation in sedimentary sequences, and well-constrained biological origins.[4] Following the established frameworks of global precipitation isotope changes, leaf wax δD effectively tracks aridity trends in tropics through the "amount effect" and heavily depends on temperature in Arctic regions.[5-8] Yet in the Asian monsoon region — the world's largest monsoon system — leaf wax δD interpretation remains unclear.

Through decades, leaf wax δD records from loess, peats and lake sediments have been increasingly established in the Asian monsoon regions over the Holocene.[9-15] They display spatially discordant patterns, which cannot be simply explained by differences in monsoon subsystems, climatic zones, nor sedimentary types. Interestingly, stalagmite $\delta^{18}O$ records exhibit remarkable spatial coherence across the Asian monsoon domain during the Holocene, considered as integrative responses to large-scale circulation dynamics.[16,17] This disparity exposes a fundamental knowledge gap — How climatic forcings operate on leaf wax δD to generate the divergent patterns? Addressing the issue is complicated by the multifaceted nature of leaf wax δD signals.

PCA offers a robust approach for disentangling signal mixtures and extracting dominant drivers.[18] Leaf wax δD records from peat deposits in the monsoon regions of China over the Holocene present an ideal case for PCA applications.[19] Peat deposits are highly sensitive to hydroclimate fluctuations. They are also rich in organic matter, which is beneficial for biomarker analysis. Moreover, they mainly consist of in-situ peat-forming plants, providing strong source constraints. Additionally, peat deposits are widely distributed in monsoonal China, ensuring regional representativeness.

In this study, we focus on well-dated Holocene peat sequences from the core monsoon regions of China, which allows clearer attribution of leaf wax δD variations to monsoon dynamics. Through the systematic application of PCA to these isotopic records, we aim to achieve three primary objectives: (1) Signal extraction — isolating the common signatures embedded in leaf wax δD records; (2) mechanistic clarification — identifying the dominant controls governing isotopic variability; and (3) comprehensive evaluation — linking PCs with isotopic processes as well as conducting proxy and regional comparisons. By bridging this critical knowledge gap, we advance the interpretation of leaf wax δD as a paleohydrological proxy in monsoon systems, with implications for understanding past hydroclimate evolution and informing modern water resource management under the context of accelerating climate changes.

DATA AND METHODS

Record compilation

In this study, peat leaf wax δD records were selected according to the following criteria. First, considering 8.2 and 4.2 kyr BP are recognized as the demarcation boundaries of the Holocene, the selected records should span a time period extending beyond the interval from 8.2 to 4.2 kyr BP. This ensures the capture of key transitions throughout the Holocene. Second, following the reference by Gao et al.,[20] a minimum of five Accelerator Mass Spectrometry (AMS) ^{14}C data points were required across the sediment cores over the Holocene. The AMS ^{14}C dating method is crucial for accurately determining the age of the sediment layers, and an adequate number of such data points ensured robust chronological control over the leaf wax δD records. Third, to avoid overlooking crucial climatic information, the average temporal resolution of the records was required to be at least 0.5 kyr per sample. This resolution is necessary to capture detailed fluctuations in leaf wax δD values, which could be related to centennial-scale climate changes.

In total, 8 records met these requirements (Figures 1 & S1, Table S1). Geographically, these sites cover a wide spatial range (25°~43° N; 99°~127° E), encompassing the core regions influenced by the Indian summer monsoon (ISM) and the East Asian summer monsoon (EASM).[21] Climatologically, they experience varying monsoon influence and divergent moisture changes. To optimize analytical efficiency while preserving climatic signals, we prioritized the HN2024 record over the HN2009 dataset,[12,22] based on its representativeness and superior temporal resolution.

Data processing

Within our PCA framework, the leaf wax δD time series of each site is treated as a distinct variable, with individual time points functioning as samples. This configuration is used to identify dominant spatial patterns of variability across diverse site records over the common time period. The suitability of PCA for our dataset is confirmed by several lines of evidence: The Bartlett's Test of Sphericity ($p < 0.001$), the Kaiser-Meyer-Olkin (KMO) Measure of Sampling Adequacy (with a KMO value of 0.695), and correlation analysis (Table S2), all of which demonstrate generally significant inter-correlations among the site records.

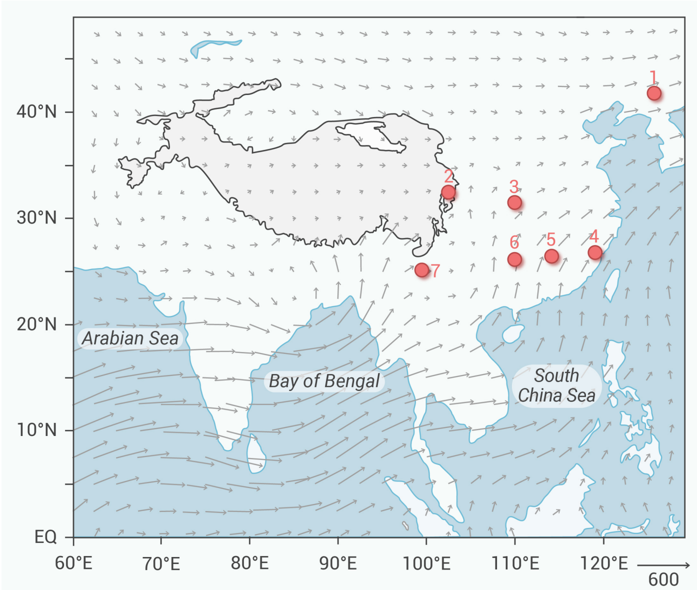

Figure 1. Distributions of the leaf wax δD records from peats in the monsoon regions of China in this study 1: Hani (HN),[12,22] 2: Hongyuan (HY),[11] 3: Dajiuhu (DJH),[9] 4: Shuizhuyang (SZY),[23] 5: Zhaogongting (ZGT),[24] 6: Shiwanggutian (SWGT),[25] and 7: Yanjiang (YJ).[26] Mean summer (June–July–August) water vapor flux vectors (kg m^{-1} s^{-1}) vertically integrated from the surface to 300 hPa during 1971–2000 CE modified after Liu et al.[27]

The leaf wax δD time series underwent standardized preprocessing in R Studio (RStudio Pbc, U.S.A.) employing linear interpolation procedures, which ensures a continuous and smooth dataset for further analysis. To determine optimal temporal resolution for PCA, we tested resolutions of 50, 100, 200, and 500 yr with SPSS 20.0 software (IBM Co., U.S.A.). The results remained consistent across all tested resolutions, suggesting that the interpolation resolution had a negligible impact on the PCA results in this study. Thus, the leaf wax δD records were analyzed at a temporal resolution of 50 yr, which approximated the minimum resolution of the leaf wax δD records.

Given that a significant proportion of the records are clustered in the middle and lower reaches of the Yangtze River, a sensitivity analysis was performed to assess potential biases arising from this spatial imbalance. The results indicate that PCA on the dataset — comprising 6 records (YJ, ZGT, SZY, DJH, HY, HN2024) — is most representative (see Text S1 & Figure S2 for details). Thus, PCA on this dataset is chosen for further analysis and discussion.

Subsequently, spectral analysis of the detrended leading principal components was performed using ACYCLE 1.2 to provide insights into the underlying climate cycles and their potential forcing mechanisms.[28] Detrending the leading principal components removed any long-term trends in the data, allowing for a more accurate identification of the cyclic components.

RESULTS

The PCA results indicate the extraction of six principal components (PCs). The cumulative contribution rate of the first three principal components, namely PC1, PC2, and PC3, exceeds 80% (Table S3). These components, each with an eigenvalue greater than 1, account for 40.5%, 23.7%, and 17.5% of the total variance, respectively (Table S3). Overall, they exhibit distinct patterns of variations (Figure S2).

PC1 exhibits an initial rise at the start of the Holocene, followed by a decreasing trend from 11.5 to 9.5 kyr BP. It then remains relatively low until 7.1 kyr BP, after which it increases until 3.5 kyr BP before declining again to 2.5 kyr BP. Records from all sites have positive loadings on PC1, with the HY site showing the highest value (Table S4 & Figure S3). PC2 displays an overall increasing trend throughout the Holocene, superimposed by frequent oscillations. The HY, HN, and SZY sites have negative loadings on PC2, while the YJ, ZGT, and DJH sites exhibit positive loadings (Table S4 & Figure S3). PC3 exhibits significant fluctuations with six pronounced peaks at 10.5, 9.2, 7.2, 6.0, 4.4, and 3.5 kyr BP. The leaf wax δD record from the DJH site has the largest loading on PC3 (Table S4 & Figure S3).

Spectral analysis of the detrended principal components reveals clear periodic oscillations (Figure S4). For PC1, millennial-scale cycles are centered around ~2,300 yr and ~1,000 yr (at a confidence level greater than 99%). PC2 shows a prominent periodicity of ~1,200 yr (at a confidence level greater than 95%). PC3 is characterized by millennial-scale cycles of ~1,500 yr and ~1,200 yr (at a confidence level greater than 99%).

DISCUSSION

Interpretations of PCs

PC1 linked to the water vapor source isotopes. During the Holocene, PC1 exhibits strong synchronicity with stalagmite $\delta^{18}O$ records from the monsoon regions of China (r^2 = 0.77, $p < 0.01$; Figure 2).[29] The coherent variations of stalagmite $\delta^{18}O$ records in China despite of the pronounced spatial heterogeneity of regional precipitation have been considered to be indicative of the upstream water vapor isotope signals, which are linked to large-scale atmospheric circulation.[16,17] Therefore, this indicates that PC1 predominantly captures isotopic signatures of the upstream water vapor source.

Supporting this interpretation, PC1 displays a striking correspondence with the leaf wax δD record from the Bay of Bengal (Figure 2).[30] This agreement is mechanistically plausible, given the Indian Ocean served as the dominant moisture source for both the ISM and EASM regions during the Holocene.[27] Notably, PC1 also parallels the reconstructed evolution of the ISM,[31] which represents the primary channel for water vapor transport from this region. Modern observational studies corroborate this link, demonstrating that precipitation isotopes across the Asian monsoon domain are significantly influenced by large-scale atmospheric dynamics, particularly in moisture-source areas, with the Indian Ocean serving as a primary source.[32,33] Additional evidence emerges from the loadings of leaf wax δD records on PC1 (Table S4 & Figure S3). First, all loadings exhibit positive values, indicating a shared climatic driver. Second, the highest loading corresponds to the HY site record, which has been shown to be especially sensitive to shifts in water vapor sourcing.[11]

Overall, the variations of PC1 closely track those of the Northern Hemi-

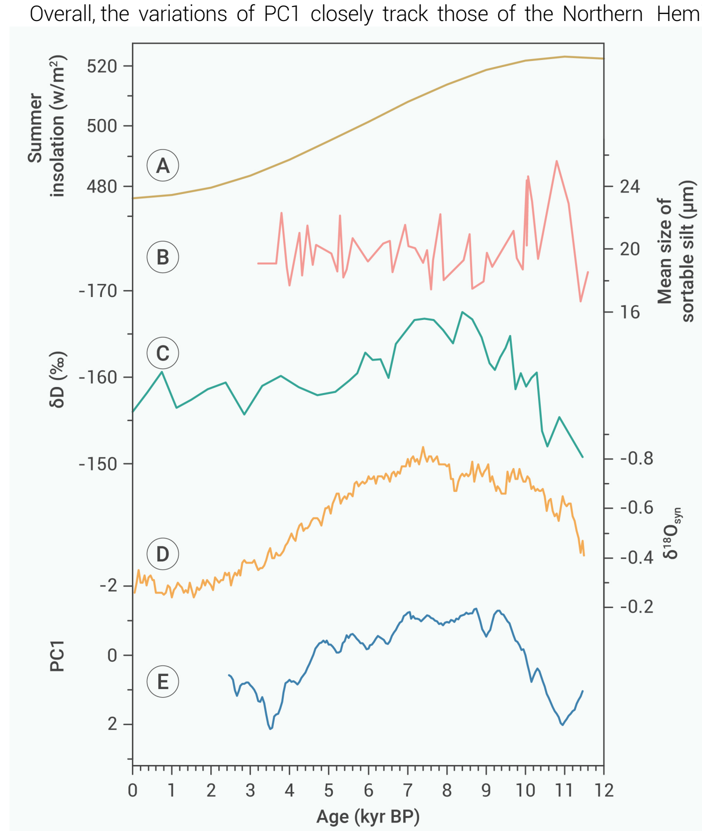

Figure 2. Comparisons of PC1 and climate records (A) 30°N summer insolation,[34] (B) the sortable silt record from northeast Atlantic, indicative of AMOC strength,[35] (C) the leaf wax δD record from the northern Bay of Bengal,[30] (D) the stacked and normalized stalagmite $\delta^{18}O$ record in China,[29] (E) PC1 in this study.

sphere summer solar insolation (Figure 2),[34] revealing solar forcing as a key influence. Furthermore, distinct ~2,300 yr and ~1,000 yr cycles are evident in PC1 (Figure S4), aligning with the well-documented Hallstatt and Eddy solar cycle, respectively.[36] Variations in solar activity can modulate the total solar irradiance received at the top of the atmosphere, with such variations superimposed on orbitally driven insolation changes.[37] Solar insolation likely modulates PC1 through two pathways: (1) By directly driving Asian monsoon intensity via land-sea thermal contrasts,[38] and (2) by regulating tropical ocean conditions that determine the isotopic composition of evaporated moisture prior to its transportation to the Asian continent.[39]

A discrepancy between summer insolation and PC1 variation during the early Holocene is noticed. This could be due to the remnant melting Laurentide Ice Sheet and resultant weakened Atlantic Meridional Overturning Circulation (AMOC), which effectively counteracted insolation-driven Asian summer monsoon (ASM) intensification (Figure 2).[40] This process concurrently altered moisture source isotopic signatures. Thus, summer insolation acts as a primary yet non-exclusive forcing on PC1.

PC2 related to the ENSO. On the whole, PC2 changes in tandem with the thermocline water temperatures anomalies (TWTA) in the Indo-Pacific warm pool (IPWP) (Figure 3).[41] The Pacific warm pool subsurface heat sequestration plays a central role in modulating the Walker Circulation and ENSO activity during the Holocene.[41] Specifically, Earth's orbital parameters—particularly precession-driven variations in solar insolation across mid-to-low latitudes — can ultimately regulate long-term changes in the west-east thermal structure of the equatorial Pacific, as well as the associated atmosphere-ocean coupling systems (i.e., ENSO and the Walker Circulation). This regulation occurs via their influence on heat transfer from subsurface circulation to the thermocline within the Warm Pool. From the early to the middle Holocene, the accumulation of heat in the subsurface layer of the Warm Pool eventually led to the suppression of ENSO activity during the middle Holocene. During the late Holocene, due to the gradual decline of the TWTA, the ENSO frequency increases significantly with a El Niño-like mean state (Figure 3).[42,43]

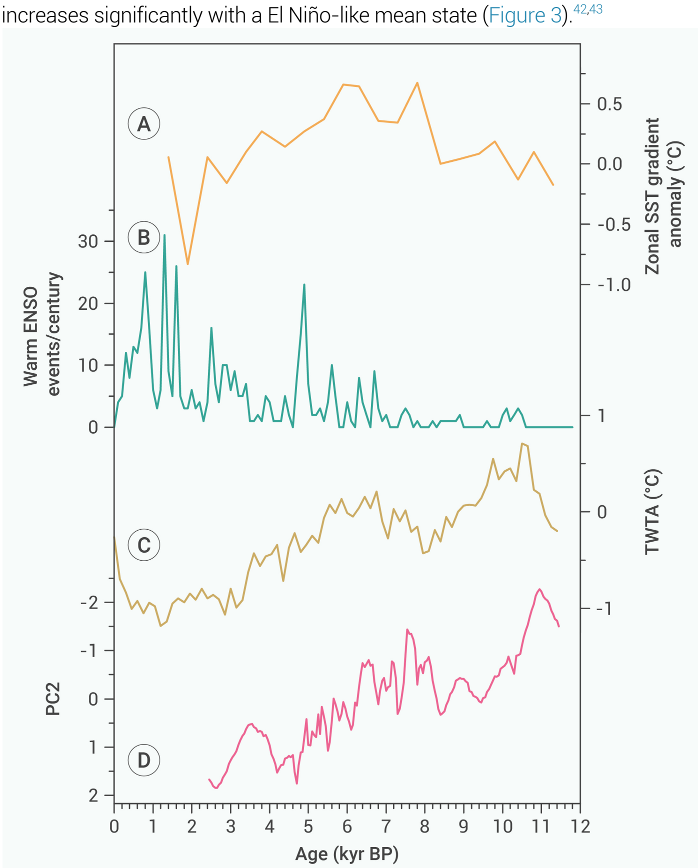

Figure 3. Comparisons of PC2 and climate records (A) Zonal SST gradient anomaly relative to the Late Holocene, calculated as the difference in SSTs between the western Pacific and eastern Pacific,[42] (B) number of warm ENSO events in 100-yr non overlapping windows,[43] (C) TWTA in the IPWP,[41] (D) PC2 in this study.

The ENSO is essentially a manifestation of the West-East Pacific SST gradients, which significantly influences the ASM in a non-linear manner, mainly through its control over the Western Pacific Subtropical High (WPSH).[44] Specifically, warming (cooling) of the SST in the eastern Pacific is typically associated with an (a) El Niño-like (La Niña-like) phase of ENSO. This tends to strengthen (weaken) the WPSH, leading to its southwestward extension (northeastward retreat).[45,46] These shifts in the WPSH, in turn, govern the spatiotemporal distribution of monsoon precipitation across monsoonal China. The central areas under the control of WPSH typically experience precipitation deficits due to the subsidence of air masses caused by descending motion. In contrast, more frontal precipitation occurs along its periphery, driven by the strong upward movement of air masses.[47,48]

The loadings of leaf wax δD records on PC2 mirror this dynamic (Table S4 & Figure S3). Positive values prevail in southwestern and central China, while negative values dominate in northern and southeastern China. The spatial distributions of these two categories closely resemble the precipitation heterogeneity pattern observed in the monsoon regions of China during the Holocene.[47-49] Notably, the ZGT site exhibits the highest loading on PC2, likely reflects its proximity to the southwestern edge of the central WPSH during the Holocene, a sensitive zone for ENSO-forced circulation shifts.[50] The spectral analysis further validates the dominant control of the ENSO on the variability of PC2 (Figure S4). PC2 shows a prominent ~1200 yr cycle, matching documented ENSO periodicities.[50]

PC3 associated with the North Atlantic cooling. The oscillations in PC3 display a notable synchronization with ice-drift events in the North Atlantic during the Holocene, though not in a strictly one-to-one manner (Figure 4).[51] The lack of consistent synchronicity for all events likely stems from variability in Bond event intensity, regional impact heterogeneity as well as nonlinear monsoon system response. This suggests that hydroclimate variations in the ASM regions sensitively respond to the climate instability in the North Atlantic. The presence of a distinct ~1,500 yr cycle in PC3, which matches the cyclicity in North Atlantic ice-drift records (Figure S4),[51] further reinforces this interhemispheric teleconnection.

Several mechanisms underlie this climatic relationship. Firstly, the North Atlantic cooling usually weakens the ASM.[44,52] This is partly because the development of an asymmetric Hadley cell which drives southward displacement of the Intertropical Convergence Zone (ITCZ). Moreover, extended Eurasian spring snow cover reduces land-ocean thermal gradients. Secondly, AMOC weakening during cooling events alters Pacific Walker Circulation, subsequently influencing ASM precipitation patterns.[53,54] This mechanism explains the ~1,200 yr cycle observed in PC3, which corresponds to characteristic ENSO variance (Figure S4).[50] Thirdly, the North Atlantic cooling can also affect ASM precipitation via the westerlies.[44] The "Jet Transition" hypothesis proposes that North Atlantic cooling intensifies and southward-shifts the Tibetan Plateau westerlies, which result in precipitation increases over central-eastern China and decreases over northeastern China.[55] The notably high loading at the DJH site (Table S4 & Figure S3) supports this mechanism. The sensitive response of the middle and lower reaches of the Yangtze River to North Atlantic cooling, as shown in the stalagmite record,

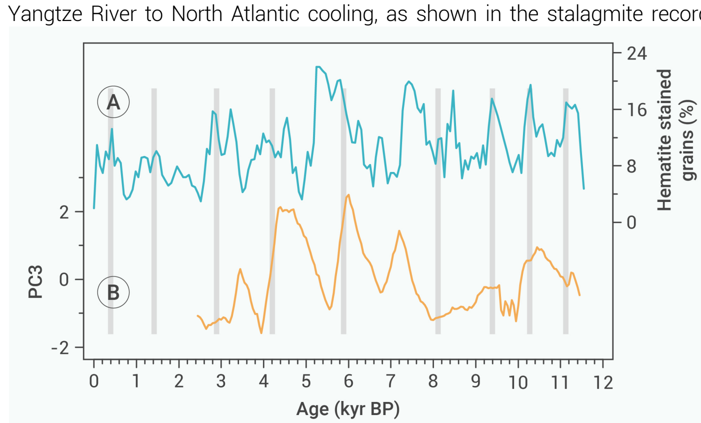

Figure 4. Comparisons of PC3 and climate records (A) ice drift records in the North Atlantic Ocean,[51] (B) PC3 in this study. The gray bar indicates the ice drift events.

has been well-explained by the "Jet Transition" hypothesis.[56] A positive loading at HN appears at first glance inconsistent with the precipitation anomaly pattern typically associated with the "Jet Transition" hypothesis under North Atlantic cooling scenarios (Table S4 & Figure S3). We propose that this pattern arises from the superimposition of multiple climatic influences, such as the ITCZ and ENSO. The specific combination and relative strength of these forcings likely varied over the Holocene.

Evaluations of PCs

PCs and isotopic processes. Building on the framework of hydrogen isotopic relationships between precipitation and leaf-wax *n*-alkanes in terrestrial plants,[2] we seek to link each principal component to specific processes within the isotopic cascade.

For PC1 (water vapor source isotopes-linked), the signal primarily reflects precipitation δD variations controlled mainly by moisture transport dynamics. For PC2 (ENSO-linked) and PC3 (North Atlantic cooling-linked), the dominant mechanisms operate through local hydroclimate modulation. Altered precipitation regimes affect evapotranspiration processes via relative humidity-controlled soil evaporation and leaf transpiration.[12] Additionally, variations in precipitation seasonality may modify the proportional contribution of isotopically distinct monsoon/non-monsoon rainfall to plant water uptake and leaf wax synthesis. Moreover, it may further affect the composition of vegetation.

Relatively minor impacts from plant types observed in this study is consistent with the individual leaf wax δD records from peatlands in the monsoon regions of China.[9,23,26] This phenomenon may partly arise from the fact that the persistent waterlogged, acidic, and nutrient-poor conditions of peatland ecosystems inherently restrict plant taxonomic diversity. Alternatively, it could be attributed to the integration of signals at the ecosystem scale in peat deposits, rather than the preservation of species-specific signatures. Notably, recent work in China based on both natural observations and experimental evidence demonstrate that the biosynthetic hydrogen isotopic fractionation for terrestrial plants is relatively constant and near -153‰.[57]

Proxy and regional comparisons. A key finding of this study is the observed covariation between PC1 and stalagmite $\delta^{18}O$ records from the monsoon regions of China during the Holocene (Figure 2). This alignment partially — if not fully — resolves the discrepancies previously reported between leaf wax δD and stalagmite $\delta^{18}O$ records in the region. Based on the PCA results, we tentatively propose that their divergence may partly stem from moisture-sensitive biological processes — such as evapotranspiration and the synthesis timing of leaf waxes — which are less prominent in stalagmite $\delta^{18}O$ records.

To further provide context on regional differences, this study is compared with a recent PCA investigation of lake sediment leaf wax δD records on the Tibetan Plateau,[20] which revealed both parallels and key differences. Specifically, precipitation δD dominates leaf wax δD in both regions (PC1), but westerly influences emerge as PC2 on the Tibetan Plateau, contrasting with the dominant role of ENSO dynamics (PC2) in our core monsoon records. The impacts of North Atlantic cooling events (PC3) are evident in both regions.

CONCLUSION

To deepen the understanding of leaf wax δD signals in the Asian monsoon regions, we systematically compiled and analyzed available peat records across monsoonal China over the Holocene using PCA. Three leading principal components were extracted and interpreted in detail. PC1 is strongly associated with water vapor source isotopes. PC2 and PC3 are linked to ENSO and North Atlantic cooling, respectively, which plays a pivotal role in shaping the spatiotemporal patterns of regional precipitation in the monsoon regions of China. These PCs well correspond to the specific processes within the isotopic cascade. The PCA results highlight that while Northern Hemisphere solar insolation provides the fundamental control, both high- and low-latitude climate systems modulate the isotopic signals. These findings also offer new insights into resolving the discrepancies between leaf wax δD and stalagmite $\delta^{18}O$ records in the ASM regions during the Holocene. Given the observed covariation between PC1 and stalagmite $\delta^{18}O$ records, we tentatively attribute the differences primarily to the moisture-sensitive biological processes—such as evapotranspiration and the synthesis timing of leaf wax.

REFERENCES

1. Bowen G. J., Cai Z., Fiorella R. P., et al. (2019). Isotopes in the water cycle: Regional-to global-scale patterns and applications. *Annu. Rev. Earth Pl. Sc.* 47:453–479. DOI:10.1146/annurev-earth-053018-060220
2. Sachse D., Billault I., Bowen G. J., et al. (2012). Molecular paleohydrology: Interpreting the hydrogen-isotopic composition of lipid biomarkers from photosynthesizing organisms. *Annu. Rev. Earth Pl. Sc.* 40:221–249. DOI:10.1146/annurev-earth-042711-105535
3. McFarlin J. M., Axford Y., Masterson A. L., et al. (2019). Calibration of modern sedimentary δ^2H plant wax-water relationships in Greenland lakes. *Quat. Sci. Rev.* 225:105978. DOI:10.1016/j.quascirev.2019. 105978
4. Inglis G. N., Bhattacharya T., Hemingway J. D., et al. (2022). Biomarker approaches for reconstructing terrestrial environmental change. *Annu. Rev. Earth Pl. Sc.* 50:369–394. DOI:10.1146/annurev-earth-032320-095943
5. Garcin Y., Schefuß E., Dargie G. C., et al. (2022). Hydroclimatic vulnerability of peat carbon in the central Congo Basin. *Nature* 612:277–282. DOI:10.1038/s41586-022-05389-3
6. Maloney A. E., Nelson D. B., Richey J. N., et al. (2019). Reconstructing precipitation in the tropical South Pacific from dinosterol $^2H/^1H$ ratios in lake sediment. *Geochim. Cosmochim. Ac.* 245:190–206. DOI:10.1016/j.gca. 2018.10.028
7. Zhao B., Russell J. M., Blaus A., et al. (2024). Tropical Andean climate variations since the last deglaciation. *Proc. Natl. Acad. Sci. USA* 121:e2320143121. DOI:10.1073/pnas.2320143121
8. Shanahan T. M., Hughen K. A., Ampel L., et al. (2013). Environmental controls on the $^2H/^1H$ values of terrestrial leaf waxes in the eastern Canadian Arctic. *Geochim. Cosmochim. Ac.* 119:286–301. DOI:10.1016/j.gca.2013.05.032
9. Huang X., Pancost R. D., Xue J., et al. (2018). Response of carbon cycle to drier conditions in the mid-Holocene in central China. *Nat. Commun.* 9:1369. DOI:10.1038/s41467-018-03804-w
10. Sarkar S., Prasad S., Wilkes H., et al. (2015). Monsoon source shifts during the drying mid-Holocene: Biomarker isotope based evidence from the core 'monsoon zone' (CMZ) of India. *Quat. Sci. Rev.* 123:144–157. DOI:10.1016/j. quascirev.2015.06.020
11. Seki O., Meyers P. A., Yamamoto S., et al. (2011). Plant-wax hydrogen isotopic evidence for postglacial variations in delivery of precipitation in the monsoon domain of China. *Geology* 39:875–878. DOI:10.1130/G32117.1
12. Wang X. and Huang X. (2024). Increasing evapotranspiration in peatlands from the monsoon regions of East China with the rapid warming during the early Holocene. *J. Hydrol.* 644:132051. DOI:10.1016/j.jhydrol.2024. 132051
13. Wang Z., Zhang F., Li X., et al. (2024). A substantial meltwater event on the northeastern Tibetan Plateau during the middle to late Holocene transition. *Quat. Sci. Rev.* 344:108996. DOI:10.1016/j.quascirev.2024.108996
14. Zhao C., Cheng J., Wang J., et al. (2021). Paleoclimate significance of reconstructed rainfall isotope changes in Asian monsoon region. *Geophys. Res. Lett.* 48:e2021GL092460. DOI:10.1029/2021GL092460
15. Rao Z., Jia G., Li Y., et al. (2016). Asynchronous evolution of the isotopic composition and amount of precipitation in north China during the Holocene revealed by a record of compound-specific carbon and hydrogen isotopes of long-chain *n*-alkanes from an alpine lake. *Earth Planet. Sc. Lett.* 446:68–76. DOI:10.1016/j.epsl.2016.04.027
16. Cheng H., Zhang H., Zhao J., et al. (2019). Chinese stalagmite paleoclimate researches: A review and perspective. *Sci. China Earth Sci.* 62:1489–1513. DOI:10.1007/s11430-019-9478-3
17. Liu X., Liu J., Chen S., et al. (2020). New insights on Chinese cave $\delta^{18}O$ records and their paleoclimatic significance. *Earth-Sci. Rev.* 207:103216. DOI:10.1016/j.earscirev.2020.103216
18. Lever J., Krzywinski M. and Altman N. (2017). Principal component analysis. *Nat. Methods* 14:641–642. DOI:10.1038/nmeth.4346
19. Chambers F. M., Booth R. K., Vleeschouwer F. D., et al. (2012). Development and refinement of proxy-climate indicators from peats. *Quatern. Int.* 268:21–33. DOI:10.1016/j.quaint.2011.04.039
20. Gao X., Sun Z., Hou X., et al. (2024). Integrating paleolimnological hydrogen and oxygen isotope records during the Holocene the Tibetan Plateau. *Global Planet. Change* 236:104432. DOI:10.1016/j.gloplacha.2024.104432
21. Wang B., Clemens S. C. and Liu P. (2003). Contrasting the Indian and East Asian monsoons: Implications on geologic timescales. *Mar. Geol.* 201:5–21. DOI:10.1016/S0025-3227(03)00196-8
22. Seki O., Meyers P. A., Kawamura K., et al. (2009). Hydrogen isotopic ratios of plant wax *n*-alkanes in a peat bog deposited in northeast China during the last 16 kyr. *Org. Geochem.* 40:671–677. DOI:10.1016/j.orggeochem.2009.03. 007
23. Wang X., Huang X., Zhao H., et al. (2022). Abrupt drying on the Southeast coast of China during the mid - to - late Holocene transition. *Geophys. Res. Lett.* 49:e2022GL100257. DOI:10.1029/2022GL100257
24. Huang X., Zhang H., Griffiths M. L., et al. (2023). Holocene forcing of East Asian hydroclimate recorded in a subtropical peatland from southeastern China. *Clim. Dynam.* 60:981–993. DOI:10.1007/s00382-022-06333-x
25. Wang X., Huang X., Dirk S., et al. (2016). Molecular paleoclimate reconstructions over the last 9 ka from a peat sequence in South China. *Plos One* 11:e0160934. DOI:10.1371/journal.pone.0160934
26. Wang X., Huang X. and Sachse D. (2023). Two-phase hydrological changes during

the mid-to late Holocene transition in Southwest China. *Quat. Sci. Rev.* **322**:108432. DOI:10.1016/j.quascirev.2023.108432
27. Liu J., Chen J., Zhang X., et al. (2015). Holocene East Asian summer monsoon records in northern China and their inconsistency with Chinese stalagmite $\delta^{18}O$ records. *Earth-Sci. Rev.* **148**:194–208. DOI:10.1016/j.earscirev.2015. 06.004
28. Li M., Hinnov L. and Kump L. (2019). Acycle: Time-series analysis software for paleoclimate research and education. *Comput. Geosci.* **127**:12–22. DOI:10.1016/j.cageo.2019.02.011
29. Yang X., Yang H., Wang B., et al. (2019). Early-Holocene monsoon instability and climatic optimum recorded by Chinese stalagmites. *Holocene* **29**:1059–1067. DOI:10.1177/0959683619831433
30. Contreras-Rosales L. A., Jennerjahn T., Tharammal T., et al. (2014). Evolution of the Indian summer monsoon and terrestrial vegetation in the Bengal region during the past 18 ka. *Quat. Sci. Rev.* **102**:133–148. DOI:10.1016/j. quascirev.2014. 08.010
31. Chen F., Chen J., Huang W., et al. (2019). Westerlies Asia and monsoonal Asia: Spatiotemporal differences in climate change and possible mechanisms on decadal to sub-orbital timescales. *Earth-Sci. Rev.* **192**:337–354. DOI:10.1016/j.earscirev.2019.03.005
32. Cai Z., Tian L. and Bowen G. J. (2018). Spatial-seasonal patterns reveal large-scale atmospheric controls on Asian Monsoon precipitation water isotope ratios. *Earth Planet. Sc. Lett.* **503**:158–169. DOI:10.1016/j.epsl.2018. 09.028
33. Wu H., Fan H., Lei R., et al. (2023). Atmospheric processes control the stable isotopic variability of precipitation in the middle–lower reaches of the Yangtze River Basin, East Asian monsoon region. *J. Hydrol.* **623**:129835. DOI:10.1016/j.jhydrol.2023.129835
34. Berger A. and Loutre M. F. (1991). Insolation values for the climate of the last 10 million years. *Quat. Sci. Rev.* **10**:297–317. DOI:10.1016/0277-3791(91)90033-Q
35. Praetorius S. K., McManus J. F., Oppo D. W., et al. (2008). Episodic reductions in bottom-water currents since the last ice age. *Nat. Geosci.* **1**:449–452. DOI:10.1038/ngeo227
36. Soon W., Velasco Herrera V. M., Selvaraj K., et al. (2014). A review of Holocene solar-linked climatic variation on centennial to millennial timescales: Physical processes, interpretative frameworks and a new multiple cross-wavelet transform algorithm. *Earth-Sci. Rev.* **134**:1–15. DOI: 10.1016/j.earscirev.2014.03. 003
37. Zhang W., Yan H., Dodson J., et al. (2018). The 9.2 ka event in Asian summer monsoon area: The strongest millennial scale collapse of the monsoon during the Holocene. *Clim. Dynam.* **50**:2767-2782. DOI:10.1007/s00382-017-3770-2
38. Cheng H., Edwards R. L., Sinha A., et al. (2016). The Asian monsoon over the past 640,000 years and ice age terminations. *Nature* **534**:640–646. DOI:10.1038/nature18591
39. Wang Q., Zhao K., Wang Y., et al. (2024). Orbital- and millennial-scale hydroclimate changes in central China during the last glacial period. *Quat. Sci. Rev.* **337**:108802. DOI:10.1016/j.quascirev.2024.108802
40. Chen F., Xu Q., Chen J., et al. (2015). East Asian summer monsoon precipitation variability since the last deglaciation. *Sci. Rep.* **5**:11186. DOI:10.1038/srep11186
41. Dang H., Jian Z., Wang Y., et al. (2020). Pacific warm pool subsurface heat sequestration modulated Walker circulation and ENSO activity during the Holocene. *Sci. Adv.* **2020**:eabc0402. DOI:10.1126/sciadv.abc0402
42. Koutavas A. and Joanides S. (2012). El Niño–Southern Oscillation extrema in the Holocene and Last Glacial Maximum. *Paleoceanography* **27**:PA4208. DOI:10.1029/2012PA002378
43. Moy C. M., Seltzer G. O., Rodbell D. T., et al. (2002). Variability of El Niño/Southern Oscillation activity at millennial timescales during the Holocene epoch. *Nature* **420**:162–165. DOI:10.1038/nature01194
44. Mohtadi M., Prange M. and Steinke S. (2016). Palaeoclimatic insights into forcing and response of monsoon rainfall. *Nature* **533**:191. DOI:10.1038/nature17450
45. Zhou L., Xia Y., Zhou C., et al. (2024). Sensitivity of western Pacific subtropical high to regional sea surface temperature changes. *Global Planet. Change.* **242**:104565. DOI:10.1016/j.gloplacha.2024.104565
46. Xue G., Cai Y., Zheng Y., et al. (2025). Western Pacific Subtropical High modulates regional hydroclimate changes on multiple timescales over central China. *J. Geophys. Res.:Atmos.* **130**:e2024JD042735. DOI: 10.1029/2024 JD042735
47. Rao Z., Li Y., Zhang J., et al. (2016). Investigating the long-term palaeoclimatic controls on the δD and $\delta^{18}O$ of precipitation during the Holocene in the Indian and East Asian monsoonal regions. *Earth-Sci. Rev.* **159**:292–305. DOI:10.1016/j.earscirev.2016.06.007
48. Xu H., Song Y., Cao J., et al. (2024). Heterogeneity of the East Asian rainfall influenced by solar-forced western Pacific subtropical high. *Commun. Earth Environ.* **5**:1–9. DOI:10.1038/s43247-024-01660-9
49. Chen F., Huang L., Cao D., et al. (2024). "Mega-sandwich Pattern" of interdecadal precipitation variations and its regional manifestation in the Asian summer precipitation region. *Sci. Bull.* **69**:2656–2659. DOI:10.1016/j.scib. 2024.06.026
50. Liu Z., Lu Z., Wen X., et al. (2014). Evolution and forcing mechanisms of El Niño over the past 21,000 years. *Nature* **515**:550–553. DOI:10.1038/nature13963
51. Bond G., Kromer B., Beer J., et al. (2001). Persistent solar influence on North Atlantic climate during the Holocene. *Science* **294**:2130–2136. DOI:10.1126/ science.1065680
52. Menzel P., Gaye B., Mishra P. K., et al. (2014). Linking Holocene drying trends from Lonar Lake in monsoonal central India to North Atlantic cooling events. *Palaeogeogr. Palaeoecol.* **410**:164–178. DOI:10.1016/j.palaeo.2014.05.044
53. Zhong Y., Liu Y., Du X., et al. (2024). Pacific Walker Circulation modulated millennial-scale East Asian summer monsoon rainfall variability over the past 40 kyr. *Global Planet. Change.* **245**:104676. DOI:10.1016/j.gloplacha.2024.104676
54. Zhang R., Sutton R., Danabasoglu G., et al. (2019). A review of the role of the Atlantic Meridional overturning circulation in Atlantic multidecadal variability and associated climate impacts. *Rev. Geophys.* **57**:316–375. DOI:10.1029/ 2019RG000644
55. Chiang J. C. H., Fung I. Y., Wu C.-H., et al. (2015). Role of seasonal transitions and westerly jets in East Asian paleoclimate. *Quat. Sci. Rev.* **108**:111–129. DOI:10.1016/j.quascirev.2014.11.009
56. Zhang H., Griffiths Michael L., Chiang John C. H., et al. (2018). East Asian hydroclimate modulated by the position of the westerlies during Termination I. *Science* **362**:580–583. DOI:10.1126/science.aat9393
57. Liu H., Wang S., Wang H., et al. (2023). Apparent fractionation of hydrogen isotope from precipitation to leaf wax *n*-alkanes from natural environments and manipulation experiments. *Sci. Total Environ.* **877**:162970. DOI:10.1016/j.scitotenv.2023.162970

FUNDING AND ACKNOWLEDGMENTS

This research was jointly funded by the Yunnan Province Science and Technology Department (202302AO370014, 202401BC070002), the National Natural Science Foundation of China (U20A2094), the Open Fund of the State Key Laboratory of Geomicrobiology and Environmental Changes (128-GKZ24Y637), and the Youth Talent Project of Yunnan Province. We extend our sincere gratitude to Dr. Xiuwu Wang for his assistance during the data-processing, to Dr. Bingyan Zhao for discussions on data interpretations, to Dr. Gaowen Dai for his support with the data analysis and to Prof. Xiting Liu and two anonymous reviewers for their constructive comments that have greatly improved the quality of the paper. The funders had no role in study design, data collection and analysis, decision to publish, or preparation of the manuscript.

AUTHOR CONTRIBUTIONS

Xinxin Wang: Conceptualization, Methodology, Investigation, Writing - Original Draft, Writing - Review & Editing. Xianyu Huang: Conceptualization, Methodology, Writing - Review & Editing, Project administration. Yixiao Xue: Methodology, Investigation. Jie Wu: Writing - Review & Editing. Shucheng Xie: Conceptualization, Writing - Review & Editing. All authors contributed to and approved the manuscript.

DECLARATION OF INTERESTS

The authors declare no competing interests.

DATA AND CODE AVAILABILITY

Data are available from the corresponding author upon reasonable request.

SUPPLEMENTAL INFORMATION

It can be found online at https://doi.org/10.59717/j.xinn-geo.2026.100180